Cell Proliferation

Cell Prolif. 2009, **42**, 75–82 doi: 10.1111/j.1365-2184.2008.00574.x

A color-coded orthotopic nude-mouse treatment model of brain-metastatic paralyzing spinal cord cancer that induces angiogenesis and neurogenesis

K. Hayashi*,†,‡, K. Yamauchi‡, N. Yamamoto‡, H. Tsuchiya‡, K. Tomita‡, M. Bouvet†, J. Wessels§ and R. M. Hoffman*,†

*AntiCancer, Inc., San Diego, CA, USA, †Department of Surgery, University of California, San Diego, San Diego, CA, USA, ‡Department of Orthopaedic Surgery, School of Medicine, Kanazawa University, Kanazawa, Ishikawa, Japan, §Department of Nephrology/Rheumatology, University of Goettingen, Goettingen, Germany

Received 29 *January* 2008*; revision accepted* 19 *April* 2008

Abstract

Objective: Cancer of the spinal cord is highly malignant and often leads to paralysis and death. A realistic mouse model would be an important benefit for the better understanding and treatment of spinal cord glioma.

Materials and methods: To develop an imageable, patient-like model of this disease, U87 human glioma tumour fragments (expressing red fluorescent protein), were transplanted by surgical orthotopic implantation into the spinal cord of nontransgenic nude mice or transgenic nude mice expressing nestin-driven green fluorescent protein (ND-GFP). In ND-GFP mice, GFP is expressed in nascent blood vessels and neural stem cells. The animals were treated with temozolomide or vehicle control.

Results: The intramedullary spinal cord tumour grew at the primary site, caused hind-limb paralysis and also metastasized to the brain. Temozolomide inhibited tumour growth ($P < 0.01$) and prevented metastasis, as well as prevented paralysis in four mice and delayed paralysis in two mice of the six tested ($P = 0.005$). In the ND-GFP-expressing host, ND-GFP cells staining positively for neuronal class III-β-tubulin or CD31, surrounded the tumour. These results suggest that the tumour stimulated both neurogenesis and angiogenesis, respectively.

Conclusion: A patient-like model of spinal cord glioma was thus developed, which can be used for the discovery of new agents, including those that inhibit invasion and metastasis of the disease as well as those that prevent paralysis.

Correspondence: R. M. Hoffman, AntiCancer, Inc., 7917 Ostrow Street, San Diego, CA 92111, USA. Tel.: +1 858 654 2555; Fax: +1 858 268 4175; E-mail: all@anticancer.com

Introduction

Cancer of the spinal cord is a highly malignant disease that often leads to paralysis and death. Intramedullary spinal cord tumours (IMSCT), an important example of spinal cord cancer, are treated by surgical resection, radiation and chemotherapy. However, the prognosis of IMSCTs, especially high-grade glioma, is among the worst of all cancers. IMSCTs usually remain asymptomatic when they are small and may increase to a considerable size before they are detected. Despite gross total resection for IMSCT, residual microscopic disease may be left in the resection bed because of its progressive infiltrative behaviour. With radical surgery and adjuvant therapy, 2-year survival rates for patients with high-grade glioma range from 0% to 40% in various studies (1,2). The main cause (over 80%) of these deaths is due to leptomeningeal metastasis (3).

Chemotherapy has been used in the treatment of IMSCT, but overall efficacy needs to be confirmed in larger studies. IMSCTs are relatively rare, accounting for only 5–10% of all central nervous system tumours (4). No large chemotherapy trial has been carried out for them. Because of its poor prognosis, development of an adequate IMSCT model is needed for testing new chemotherapeutic agents and for further understanding of the natural history and biology of the disease.

There are previous reports on IMSCT models in dog, rabbit and rat, but not in mice (5–7). In this report, we describe an orthotopic red fluorescent protein (RFP) imaging IMSCT model with the U87 human high-grade glioma cell line in nude mice, which leads to progressive paralysis. The efficacy of chemotherapy was also evaluated.

In addition to standard nude mice, transgenic nude mice were used as hosts in which green fluorescent protein (GFP) is driven by a regulatory element of the stem cell marker nestin (ND-GFP). We observed ND-GFP host cells gathered around the glioma cells transplanted in the spinal cord and confirmed that these cells comprised both neural and endothelial cells. Using this colour-coded orthotopic model of IMSCT, we demonstrate its usefulness in understanding the biology of the disease and its use as a treatment model.

Materials and methods

RFP vector production

The RFP (DsRed-2) gene (BD Biosciences Clontech, Palo Alto, CA, USA) was inserted in the retroviral-based mammalian expression vector pLNCX (BD Biosciences Clontech) to form the pLNCX DsRed-2 vector. Production of retrovirus resulted from transfection of pLNCX DsRed-2 into PT67 packaging cells, which produce retroviral supernatants containing the DsRed-2 gene. Briefly, PT67 cells were grown as monolayers in DMEM supplemented with 10% foetal calf serum (FCS; Gemini Biological Products, Calabasas, CA, USA). Exponentially growing cells (in 10-cm dishes) were transfected with 10 μg expression vector using LipofectAMINE PLUS Reagent (Life Technologies, Grand Island, NY, USA). Transfected cells were replated 48 h after transfection and 100 μg/mL G418 was added 7 h after transfection. Two days later, the medium was changed and the level of G418 increased to 200 μg/mL. After 25 days of drug selection, surviving colonies were visualized using a fluorescence microscope, and RFP-positive colonies were isolated. Several clones were selected and expanded into cell lines after virus titrating on the 3T3 cell line.

RFP gene transduction of tumour cell lines

For RFP gene transduction, 70% confluent U87 human glioma cells were incubated with a 1 : 1 precipitated mixture of retroviral supernatant of PT67 cells and RPMI 1640 or other culture media (Life Technologies) containing 10% FCS (Gemini Biological Products) for 72 h. Fresh medium was replenished at this time. Cancer cells were harvested with trypsin/ethylenediaminetetraacetic acid (EDTA) and were subcultured at a ratio of 1 : 15 into selective medium, which contained 50 μg/mL G418. To select brightly fluorescent cells, the level of G418 was increased to 800 μg/mL in a stepwise manner. Clones expressing RFP were isolated with cloning cylinders (Bel-Art Products, Pequannock, NJ, USA) by trypsin/EDTA and were amplified and transferred by conventional culture methods in the absence of selective agent.

Orthotopic transplantation of RFP-expressing U87 human glioma cells

Female nude mice (4–6 weeks old) were used as hosts for the U87-RFP human glioma cell line. The mice were anaesthetized before surgery with a ketamine mixture (10 μL ketamine HCl, 7.6 μL xylazine, 2.4 μL acepromazine maleate and 10 μL H_2O) via subcutaneous injection. RFP-expressing U87 cells (1×10^6) were injected into the subcutaneous tissue with a 0.5-mL, 28-G latex-free syringe (Tyco Health Group LP, Mansfield, MA, USA). Fragments (0.5 mm) from the resulting subcutaneous tumour, stably expressing RFP, were implanted by surgical orthotopic implantation into the spinal cord. A midline incision, approximately 2 cm long, was made over the midthoracic spine, and then subperiosteal dissection of the paravertebral muscles was performed. The spinous process and bilateral lamina of one midthoracic level vertebra (T7) were removed using a blade, to expose the dura matter. A 28-G needle was inserted into the dorsal centre of the spinal cord, avoiding blood vessel injury, to create a 0.5-mm longitudinal incision. The U87-RFP tumour fragment was implanted into this incision of the spinal cord. All tumour pieces were determined to be stably expressing RFP. The muscles, fascia and skin were closed with a 6–0 surgical suture. After recovery, animals were returned to their cages. Each animal was subsequently evaluated twice a day for any neurological deficit.

Chemotherapy using the IMSCT model

Two days after transplantation, mice were treated daily with temozolomide (100 mg/kg, i.p.) for 5 days. Five mice were treated with temozolomide and five mice were used as the control group. Temozolomide was dissolved in 30% dimethyl sulphoxide and 70% normal saline; control mice received vehicle only. The dose was determined using information from previous reports (7,8). Animals were sacrificed by administration of high-dose ketamine mixture 4 weeks after transplantation. Following euthanasia, the thorax was rapidly opened, and a cannula was inserted into the left ventricle of the heart and formalin (10%) was pumped through the animal's circulation. Approximately five levels of laminae, centred on the site of tumour transplantation, were removed. The skull was opened and the brain was excised en bloc. Fluorescence imaging of the spinal cord and brain was performed using an Olympus OV100 Small Animal Imaging System (Olympus Corp., Tokyo, Japan). The primary tumour size [RFP area (mm^2)] was measured and expressed as mean ± standard error. The two-tailed Student's *t*-test was used for statistical analysis. The dissected cord and brain were placed in formalin (10%). After a 1 week fixation, they were processed, sectioned and stained with haematoxylin and eosin.

Functional evaluation of hind limbs to determine degree of paralysis

Functional evaluation of hind-limb strength was assessed using the Basso, Bresnahan and Beattie (BBB) scale (9). Mice were placed in an open field testing area and were

observed for 5 min. Locomotion was rated using the BBB locomotor scale. The BBB scale ranges from 21 to 0 (21 means consistent plantar stepping and coordinated gait, consistent toe clearance, predominant paw position is parallel throughout stance, consistent trunk stability, and tail consistently up; zero means no observable hind-limb movement). All animals had been tested preoperatively to ensure a baseline locomotor rating of 21. After tumour transplantation, the animals were tested at least once every other day. Two different observers were randomly assigned to score the animals' motor function. Results of the BBB score are expressed as the mean. When the functional BBB score of an animal was 0, euthanasia was performed. The experiment was concluded by day 60, and all animals were sacrificed at this time. Kaplan–Meier curves were used to demonstrate survival distribution. The log-rank test was used to compare survival data between the two groups. Each group consisted of six mice.

ND-GFP transgenic nude mice

Interaction of the RFP-glioma and host ND-GFP-expressing cells in the spinal cord was observed by fluorescence microscopy. ND-GFP transgenic C57/B6 mice express GFP under control of the nestin regulatory elements (10,11). Previously, the ND-GFP gene had been crossed into nude mice with C57/B6 background, to obtain ND-GFP nude mice (12). Orthotopic tumour transplantation was performed by the methods described above. Ten days after tumour transplantation, mice were sacrificed and the thoracic spinal cord was dissected. Tumour and ND-GFP cell interaction was observed by fluorescence microscopy. Excised spinal cord, including the tumour, was flattened on a glass slide, which enabled tissue structure to be seen. To compare the effect of age, three 6-week-old (young) and three 16-week-old (old) mice had been used. Mean GFP intensity (intensity/mm^2) around the tumour was measured and intensity in each group was expressed as mean ± standard error. Statistical analysis was performed using the two-tailed Student's *t*-test.

Fluorescence imaging

The Olympus OV100 Small Animal Imaging System (Olympus Corp.), containing an MT-20 light source (Olympus Biosystems, Planegg, Germany) and DP70 CCD camera (Olympus), was used for imaging live mice. High-resolution images were captured directly on a personal computer (Fujitsu Siemens Computers, Munich, Germany). Images were processed for contrast and brightness and were analysed with the use of Paint Shop Pro 8 and CellR (Olympus Biosystems).

Immunohistochemical staining

At sacrifice, the tumour including surrounding tissue, was excised and fixed with 4% paraformaldehyde. To detect neural cells, immunofluorescence was performed with anti-III-β-tubulin monoclonal antibody (1 : 500, Tuj1 clone; Covance Research Products, Berkeley, CA, USA) as primary antibody and Alexa Fluor 633-conjugated rabbit anti-mouse (1 : 200; Molecular Probes) as secondary antibody. Images were obtained with the IV100 Laser Scanning Microscope (Olympus Corp.) using 488-, 561- and 633-nm lasers. High-resolution images were captured directly on a personal computer (Dell Inc., Minneapolis, MN, USA).

To detect endothelial cells, frozen sections (10 μm) were mounted on slides. CD31 in the frozen sections was detected with an anti-rat immunoglobulin horseradish peroxidase detection kit (BD Pharmingen, San Diego, CA, USA) following the manufacturer's instructions. Primary antibody used was CD31 monoclonal antibody (1 : 50). Substrate-chromogen 3,3′-diaminobenzidine staining was used for antigen staining. Anti-CD31 monoclonal antibody (CBL1337) was purchased from Chemicon (Temecula, CA, USA).

Results and discussion

Growth and metastasis of spinal cord glioma

Four weeks after transplantation, spinal cords were exposed by laminectomy. The RFP-expressing glioma in the spinal cord was observed using fluorescence imaging (Fig. 1a). The skull was opened and the brain was excised en bloc. Brain metastases were detected even though they were small (Fig. 1b,c); they were found mainly around the brain stem and in leptomeninges at the basilar sulcus.

Efficacy of chemotherapy on tumour growth and metastasis

Primary tumour size was significantly reduced by temozolomide treatment compared to untreated controls (0.55 ± 1.1 vs. 9.7 ± 4.1 mm^2, $P < 0.01$, $n = 5$ for each group) and brain metastases were found only in the control group (60%). Histological analysis of the control group showed aggressive tumour invasion in the spinal cord. In contrast, temozolomide-treated animals showed mostly scar tissue after tumour transplantation (Fig. 1d,e).

Efficacy of chemotherapy on hind-limb paralysis

Untreated mice showed progressive paralysis beginning at 14 days after U87 glioma transplantation. The untreated

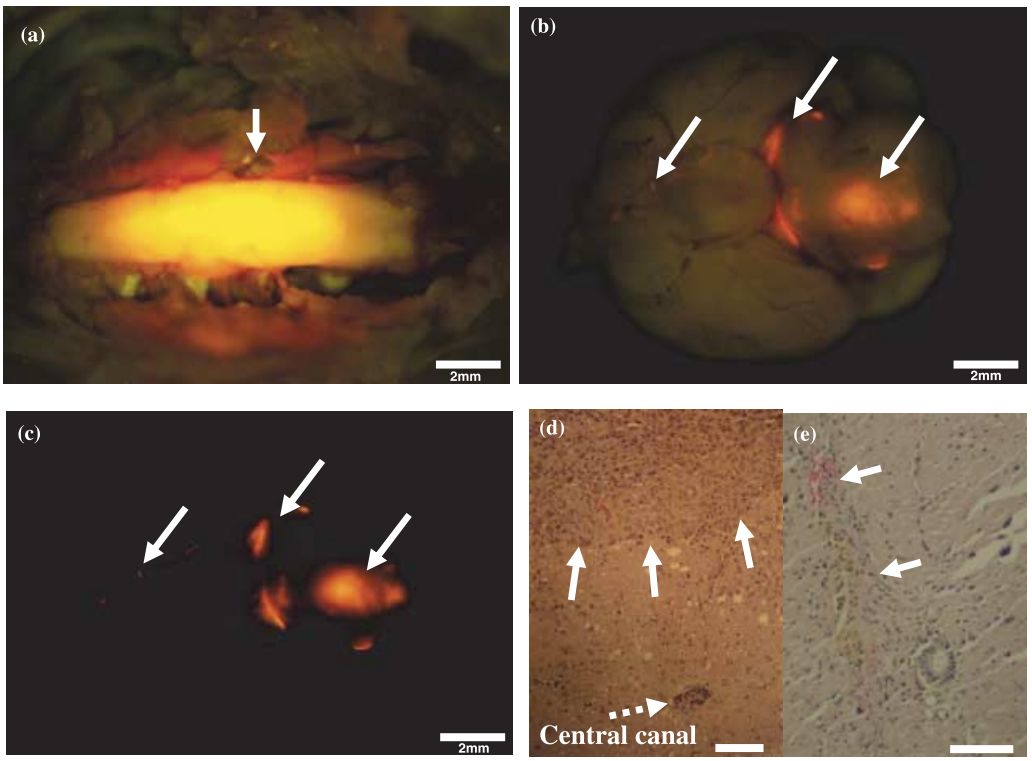

Figure 1. Surgical orthotopic implantation of human glioma into the spinal cord in nude mice. A 28-G needle was inserted into the dorsal centre of the spinal cord to create a 0.5-mm longitudinal incision. Tumour pieces were implanted into the incision in the spinal cord. After transplantation, tumour pieces were subsequently observed to remain embedded *in situ*. (a) Four weeks after transplantation in the control group, the spinal cord was exposed by laminectomy. The tumour (arrow) expressing red fluorescent protein (RFP) growing in the spinal cord was observed under fluorescent light (excitation 460–490, emission > 510). (b) The skull was opened and the brain was excised *en bloc*. At the base of the brain, RFP metastases are seen in the pons and the leptomeninges (arrows). (c) Same field as (a) but only RFP (excitation 545 nm, emission 570–625 nm). (d) Four weeks after tumour transplantation in the control group, the U87 glioma invaded and compressed the normal spinal cord (arrow), haematoxylin and eosin stained section. (e) In the temozolamide group, only scar tissue was observed in the transplantation site (arrow). Bars: (a–c) = 2 mm; (d) and (e) = 50 μm.

control group developed complete paralysis (BBB score = 0; Fig. 2a) between 18 and 31 days after tumour transplantation. Some of the temozolomide-treated mice started to show paralysis at approximately 35 days after transplantation and four mice were still not paralysed at 60 days (Fig. 2a). Temozolomide-treated mice survived without complete paralysis for at least 45 days (Fig. 2b). There was a significant delay to onset or complete inhibition of paralysis in the treated animals (log rank statistic 8.37, $P < 0.005$).

Angiogenesis and neurogenesis of the spinal cord glioma

In frozen sections of normal spinal cord, ND-GFP-positive cells were mainly seen around the central canal (Fig. 3a). Ten days after U87-RFP glioma transplantation, ND-GFP-positive cells appeared, stimulated by the tumour and started to surround it (Fig. 3b). The main stem of the ND-GFP-positive cells had many small branches and ND-GFP-positive cells appeared to originate from the cells around the central spinal cord canal (Fig. 3c–f). In young (6 week old) mice, more ND-GFP-positive cells were observed surrounding the tumour than in old (16 week) mice (Fig. 3g,h). The mean GFP intensity around the tumour in young mice was significantly higher than in old mice ($P \leq 0.05$) (Fig. 2c).

Neuronal class III-β-tubulin is a marker of neuronal cells. Some of the ND-GFP-positive cells surrounding the spinal cord glioma also expressed III-β-tubulin, indicating that some of the ND-GFP-positive cells accumulating around the tumour are of neural origin (Fig. 4a–c). Some of the ND-GFP-positive cells also appeared to be endothelial cells (Fig. 4d). CD31 is an epithelial cell marker that is commonly used to identify tumour vessels. Frozen sections showing the ND-GFP host cells and RFP-expressing U87 cells under a fluorescence microscope were compared with sister sections immunohistochemically stained for CD31. This comparison demonstrated colocalization of ND-GFP and CD31 cells (Fig. 4e.f). These results indicate that the ND-GFP cells surrounding the tumour contained both neural and endothelial types.

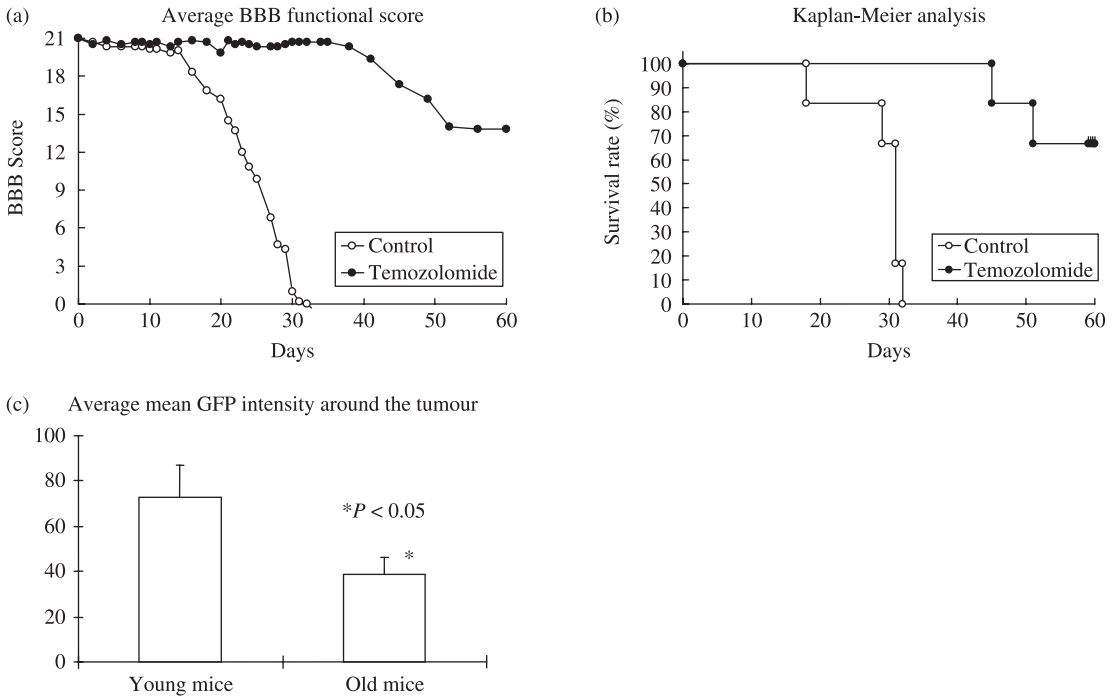

Figure 2. Efficacy of temolozomide on spinal cord glioma. (a) Basso, Bresnahan and Beattie (BBB) functional score of hind limb function; evaluation of hind-limb function was assessed using this BBB scale which ranges from 21 to 0 (21 means consistent plantar stepping and coordinated gait, consistent toe clearance, predominant paw position is parallel throughout stance, consistent trunk stability, and tail consistently up; zero means no observable hind-limb movement). After tumour transplantation, the mice were tested at least once every other day. Six mice were treated with temozolomide (100 mg/g i.p. for 5 days) and six mice were in the control group. The experiment was concluded at day 60, at which time all mice were sacrificed. Results of the BBB score are expressed as a mean. Mice in the control group showed progressive paralysis starting at 14 days after U87 glioma transplantation and eventually they all developed complete paralysis within 31 days. In the temozolomide group, some of the mice started to show paralysis by day 35 but four mice did not show any severe paralysis 60 days after transplantation. (b) Kaplan–Meier analysis. When the functional BBB score of an animal was 0, euthanasia was performed. Kaplan–Meier curves were used to demonstrate survival distribution. The log-rank test was used to compare survival data between two groups. Mice in the temozolomide group survived at least 45 days and four mice were still alive at day 60. There was a significant difference between survival in the two groups ($P < 0.005$). (c) Average mean green fluorescent protein (GFP) intensity around the tumour. Mean GFP intensity (intensity/mm^2) around the tumour was measured with the OV100. In young mice, GFP intensity is significantly higher than in old mice (72.5 ± 14.7 vs. 38.9 ± 7.5, $P < 0.05$).

Grade 4 gliomas have multiple genetic and chromosomal abnormalities, which cause these tumours to be highly aggressive. Their cells rapidly invade, infiltrate and destroy neighbouring areas. In this report, we describe an orthotopic colour-coded imageable IMSCT glioma nude mouse model as an example of paralysing spinal cord cancer. The tumour-bearing mice developed progressive paralysis. Primary tumour and metastases were easily detected by fluorescence imaging demonstrating similarity of the natural history of the model to clinical IMSCT.

Temozolomide is the only known effective chemotherapeutic agent for cranial gliomas, and in this study the effectiveness was also confirmed in our IMSCT glioma model. Temozolomide inhibited increase in tumour size, metastasis and development of paralysis.

Co-culture experiments showed that neural precursors suppressed cancer cell proliferation. In *in vivo* studies,

Figure 3. Colour-coded imaging of tumour–host interaction in nestin-driven green fluorescent protein (ND-GFP) mice. Ten days after orthotopic transplantation of the red fluorescent protein-expressing U7 glioma into ND-GFP mice, the animals were sacrificed and the thoracic spinal cord was dissected. Cancer and host ND-GFP cell interaction was observed by fluorescence microscopy. (a) Frozen section of normal spinal cord. ND-GFP cells are mainly seen around the central canal. (b) Ten days after transplantation, ND-GFP cells appear to be stimulated by the tumour and observed to surround it. (c) Higher magnification of ND-GFP cells. Main stems of ND-GFP cells had many small branches. (d) ND-GFP cells growing into the tumour. (e) ND-GFP cells seemed to originate from pre-existing cells around the central canal. (f) Tissue flattening enabled visualization of fine fibrous structures. (g) In young mice, more ND-GFP cells surround the tumour than in old mice. (h) In old mice, fewer ND-GFP cells surround the tumour. Bars: (a), (b) and (f) = 100 μm; (e) = 1 mm; (g) and (h) = 200 μm.

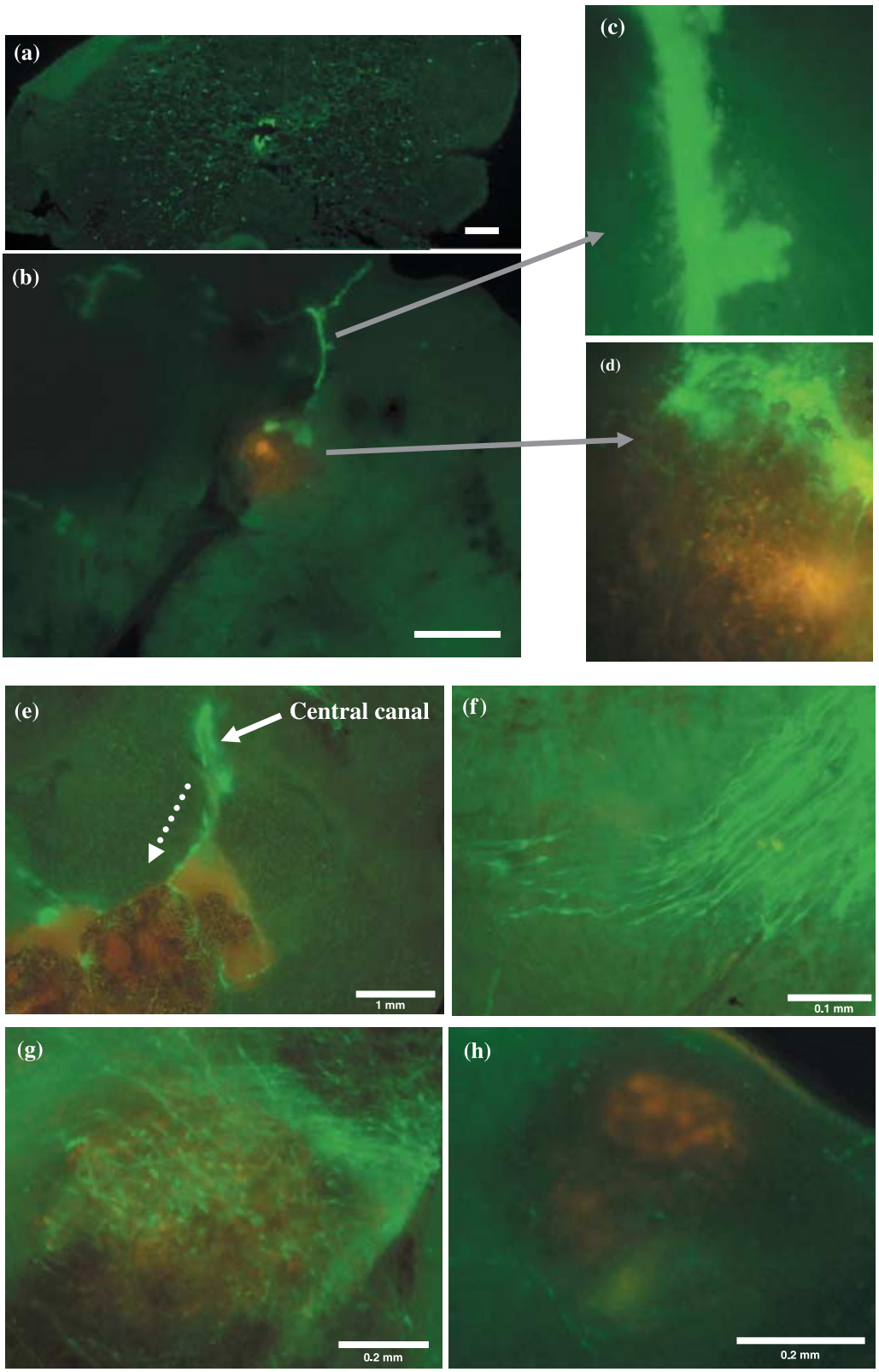

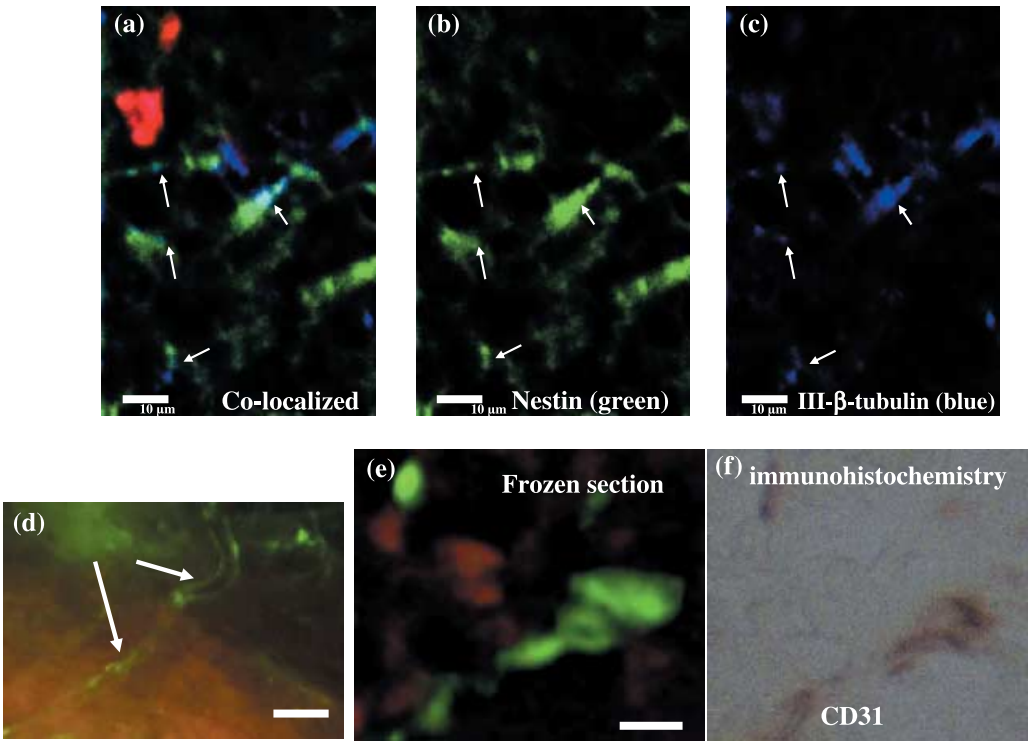

Figure 4. Angiogenesis and neurogenesis in spinal cord glioma. (I) Immunofluorescence of neuronal class III-β-tubulin. U87-RFP was transplanted in the spinal cord of nestin-driven green fluorescent protein (ND-GFP) nude mice and 10 days later, the tumour including the surrounding tissue was excised. Immunofluorescence was performed with anti-III-β-tubulin monoclonal antibody as primary antibody and Alexa Fluor 633-conjugated rabbit anti-mouse as secondary antibody. Neuronal class III-β-tubulin is a marker of neuronal cells. (a) Immunofluorescence of the frozen section shows U87 glioma (red), ND-GFP cells (green) and III-β-tubulin (blue). Some ND-GFP host cells surrounding the tumour expressed III-β-tubulin indicating they are neural precursors (arrows). (b) Only ND-GFP (green). (c) Only III-β-tubulin (blue). Bars: (a–c) = 10 μm. (II) Immunohistochemical staining of CD31. (d) Flattened tumour sample in ND-GFP mice. Some ND-GFP cells appear to be a vascular component. (e) ND-GFP is visualized interacting with U87-RFP human glioma cells in a frozen section. (f) CD31 is commonly used to identify endothelial cells. Immunohistochemical staining in a sister frozen section shows CD31 colocalizing with ND-GFP. Bars: (d) = 50 μm; (e) = 10 μm.

glioma cells were transplanted into the brain of ND-GFP mice. Abundance of neural precursors associated with the tumour apparently reduced tumour size and increased survival. The stem cells appeared to have a direct anti-tumour effect. Currently, glioma therapy relies on classical treatment, such as surgery, chemotherapy and radiation (1–4,13,14). Adaptation of stem cells for treating glioma is a promising future therapy for IMSCT. The colour-coded imageable orthotopic model of IMSCT discussed here should be useful for the discovery of newer treatment modalities (including stem cells) for this disease.

In conclusion, we have developed an imageable patient-like treatment model of spinal cord cancer. Tumour growth in the spinal cord leads to paralysis of the hind limbs. The tumour also metastasized to the brain. There have been only few reports that use mouse models to study human tumours that metastasize to the brain (15–17); this makes our present model very valuable for the study of brain metastasis. Temozolomide is effective in this model against primary tumour growth in the spinal cord, paralysis and brain metastasis. Differential labelling of the tumour and host enabled us to observe that the primary tumours stimulate both blood vessel and nerve growth. The novel mouse model used here will enable a deeper understanding of spinal cord cancer, and provide a clinically relevant system for drug discovery and evaluation.

References

1 McLaughlin MP, Buatti JM, Marcus RB Jr, Maria BL, Mickle PJ, Kedar A (1998) Outcome after radiotherapy of primary spinal cord glial tumors. *Radiat. Oncol. Investig*. **6**, 276–280.
2 Shirato H, Kamada T, Hida K, Koyanagi I, Iwasaki Y, Miyasaka K, Abe H (1995) The role of radiotherapy in the management of spinal cord glioma. *Int. J. Radiat. Oncol. Biol. Phys*. **33**, 323–328.
3 Constantini S, Miller DC, Allen JC, Rorke LB, Freed D, Epstein FJ (2000) Radical excision of intramedullary spinal cord tumors: surgical morbidity and long-term follow-up evaluation in 164 children and young adults. *J. Neurosurg*. **93**, 183–193.
4 Epstein FJ, Farmer J-P (1990) Pediatric spinal cord tumor surgery. *Neurosurg. Clin. N. Am*. **1**, 569–590.

5 Caplan J, Pradilla G, Hdeib A, Tyler BM, Legnani FG, Bagley CA, Brem H, Jallo G (2006) A novel model of intramedullary spinal cord tumors in rats: functional progression and histopathological characterization. *Neurosurgery* **59**, 193–200.
6 Mavinkurve G, Pradilla G, Legnani FG, Tyler BM, Bagley CA, Brem H, Jallo G (2005) A novel intramedullary spinal cord tumor model: functional, radiological, and histopathological characterization. *J. Neurosurg. Spine* **3**, 142–148.
7 Cheng CL, Johnson SP, Keir ST, Quinn JA, Ali-Osman F, Szabo C, Li H, Salzman AL, Dolan ME, Modrich P, Bigner DD, Friedman HS (2005) Poly (ADP-ribose) polymerase-1 inhibition reverses temozolomide resistance in a DNA mismatch repair-deficient malignant glioma xenograft. *Mol. Cancer Ther*. **4**, 1364–1368.
8 Momota H, Nerio E, Holland EC (2005) Perifosine inhibits multiple signaling pathways in glial progenitors and cooperates with temozolomide to arrest cell proliferation in gliomas *in vivo*. *Cancer Res*. **65**, 7429–7435.
9 Basso DM, Beattie MS, Bresnahan JC (1996) Graded histological and locomotor outcomes after spinal cord contusion using the NYU weight-drop device versus transection. *Exp. Neurol*. **139**, 244–256.
10 Li L, Mignone J, Yang M, Matic M, Penman S, Enikolopov G, Hoffman RM (2003) Nestin expression in hair follicle sheath progenitor cells. *Proc. Natl. Acad. Sci. USA* **100**, 9958–9961.
11 Amoh Y, Li L, Yang M, Moossa AR, Katsuoka K, Penman S, Hoffman RM (2004) Nascent blood vessels in the skin arise from nestin-expressing hair follicle cells. *Proc. Natl. Acad. Sci. USA* **101**, 13291–13295.
12 Amoh Y, Yang M, Li L, Reynoso J, Bouvet M, Moossa AR, Katsuoka K, Hoffman RM (2005) Nestin-linked green fluorescent protein transgenic nude mouse for imaging human tumor angiogenesis. *Cancer Res*. **65**, 5352–5357.
13 Kawahara N, Tomita K, Shinya Y, Matsumoto T, Baba H, Fujita T, Murakami H, Kobayashi T (1999) Recapping T-Saw laminoplasty for spinal cord tumors. *Spine* **24**, 1363–1370.
14 Stupp R, Mason WP, van den Bent MJ, Weller M, Fisher B, Taphoorn MJ, Belanger K, Brandes AA, Marosi C, Bogdahn U, Curschmann J, Janzer RC, Ludwin SK, Gorlia T, Allgeier A, Lacombe D, CaiRncross JG, Eisenhauer E, Mirimanoff RO, European Organisation for Research and Treatment of Cancer Brain Tumor and Radiotherapy Groups National Cancer Institute of Canada Clinical Trials Group (2005) Radiotherapy plus concomitant and adjuvant temozolomide for glioblastoma. *N. Engl. J. Med*. **352**, 987–996.
15 Yang M, Jiang P, Sun FX, Hasegawa S, Baranov E, Chishima T, Shimada H, Moossa AR, Hoffman RM (1999a) A fluorescent orthotopic bone metastasis model of human prostate cancer. *Cancer Res*. **59**, 781–786.
16 Yang M, Jiang P, An Z, Baranov E, Li L, Hasegawa S, Al-Tuwaijri M, Chishima T, Shimada H, Moossa AR, Hoffman RM (1999b) Genetically fluorescent melanoma bone and organ metastasis models. *Clin. Cancer Res*. **5**, 3549–3559.
17 Cruz-Munoz W, Man S, Xu P, Kerbel RS (2008) Development of a preclinical model of spontaneous human melanoma central nervous system metastasis. *Cancer Res*. **68**, 4500–4505.

